JOURNAL OF MATERIALS SCIENCE 15 (1980) 2241–2252

Reduction kinetics and microstructures of Al^{3+}-containing cobalt ferrites

MICHAEL C. RAY
Monsanto Research Corporation, Miamisburg, Ohio 95392, USA

LUTGARD C. DE JONGHE
Materials and Molecular Division, Lawrence Berkeley Laboratory, University of California, Berkeley, California 94720, USA

Dense, polycrystalline $CoFe_2O_4$, $CoAl_{0.02}Fe_{1.98}O_4$, and $CoAl_{0.1}Fe_{1.9}O_4$ were reduced in flowing H_2/0.01% H_2O at temperatures between 500 and 800° C. The reactions proceeded in a topochemical fashion. The rate of advance of the reaction interface was determined by direct measurement and by thermogravimetric analysis. An anomalous decrease in the reduction kinetics was observed for $CoFe_2O_4$ around 650° C and for $CoAl_{0.02}Fe_{1.98}O_4$ at 750° C. This reaction rate anomaly could be attributed to the appearance of a wüstite-type subscale. The effect of the substitutional Al^{3+} ions was to decrease the interfacial reaction rates. In the lower temperature range, the reaction was dominated by the interface reaction. With increasing temperatures, the importance of the gas transport resistance through the porous metal product scale increased. The microstructure of the scales was examined extensively. Pronounced grain-boundary attack was observed at lower temperatures leading to the formation of a distributed reaction interface. At higher temperatures, the reaction interface was better defined. The pore structure of the scales was examined after polishing and sputter etching. While changes in the pore morphology were observed, they were not correlated with the anomalous reaction rate effects.

1. Introduction

Many problems associated with the production of energy from unconventional sources stem from the limitations on materials performance. Chemical stability is one important materials property which ultimately limits the usefulness of ceramic alloys. For oxide ceramics, rapid removal of oxygen from the lattice in a reducing environment at high temperatures is an example of an important chemical materials limitation. Ideally the resistance of oxides to gaseous reduction might be improved by the addition of an appropriate alloying element, as is common in the protection of metals against oxidation. However, the reduction of oxides proceeds in a substantially different manner from the reverse reaction, the oxidation of metals, so that direct correlation between oxidation and reduction behaviour in the presence of alloying elements does not exist. An important aspect is that the molar volume of the reduction product is significantly smaller than that of the parent material. The reduction product layer is porous and does not provide an effective barrier against further reaction. Reduction reactions can, therefore, proceed quite rapidly, compared to oxidation reactions, so that non-equilibrium effects at interfaces may be important. The detailed analysis of a reduction reaction can be quite complicated but modelling can often be done considering only three reaction resistances [1]: (1) the mass transfer resistance to flow of gas from the bulk gas stream; (2) the gas transport resistance to gas-phase diffusion through the porous product layer; (3) the interface reaction resistance. In that way the simplest, ideally topochemical reduction, can be described with fairly simple, lumped parameter models. In these treatments a number of temperature-dependant coefficients appear that may be formally associated with the three succesive individual reaction steps that were considered. It

0022–2461/80/092241–12$03.20/0

should be understood, however, that the reaction kinetic parameters cannot always be interpreted in terms of single, elementary processes. For example, gas diffusion in the porous metal layer may be a combination of molecular diffusion, Knudsen diffusion, and gas transport through the metal itself. The interface reaction, also described with a single kinetic parameter, actually involves gas absorption, desorption, associations and dissociations on the surface, and so on, as well as solid state diffusion near or in the moving reaction interface. In multi-cation oxides additional complications may arise, e.g. segregation near the interface, preferential reactions along grain boundaries, retention of unreduced material in the product scale, or sintering effects in the product scale during the course of the reduction. Kinetic measurements should, therefore, be supplementary to a microcharacterization of the reaction-product scale and of the interface region between the product layer and the unreduced bulk to further elucidate the meaning of the lumped parameters of the models.

Anomalies in reaction rates during the course of the reduction have been observed in a number of iron oxides reduced by hydrogen [2–5]. For example, Turkdogan and Vinters [2] reported an unusual temperature effect in the reduction of powdered hematite samples. Above 570° C the observed reduction rate dropped markedly. The effect appeared to be more pronounced for smaller samples. For iron oxides, the rate anomalies have been attributed to a variety of causes: product scale sintering, internal reduction and retained wüstite, and formation of a wüstite subscale above 570° C (although the observed decrease in reduction rate may occur significantly above the wüstite stability temperature). Similar reaction rate anomalies have also been observed in systems other than iron oxides. Lilius [7], for example, reported this phenomenon in the reduction of CoO, and attributed it to scale sintering. This appeared to be the only reasonable explanation for this material, since there is no possible intermediate oxide phase between CoO and cobalt metal. The lowering of reduction rates caused by sintering of the product scale has been included in the modelling work of Szekely and Evans [6]. If scale sintering is indeed responsible for the rate anomaly, a microstructural characterization should reveal a definite correlation.

It is well known that the addition of dopants to an oxide can significantly alter its physical and chemical properties. Two broad classes of dopants may be considered: interactive and non-interactive dopants. Non-interactive dopants remain as a separate, inert phase throughout the chemical reaction. The mechanisms by which such inclusions may affect the reactivity of solids were classified by Delmon [8]. These mechanisms include alteration of the diffusion paths of the reactant and product gasses, nucleation catalysis, and rate changes in adsorption or desorption of gases at the reaction interface [10–13]. Interactive dopants react chemically with either the parent or the product phase to form solid solutions or single-phase chemical compounds. The solid solution additive may alter the properties of the material by affecting the point-defect structure or by causing lattice strains and thereby creating sites for easy nucleation of the reduced phase [13]. The thermodynamic stability of the additive itself could alter the reducibility of the host material. As an example, the addition of cobalt oxide to wüstite is expected to increase the reducibility of the host material, since it will increase the alloy equilibrium oxygen parital pressure at a given temperature, as was shown in the phase diagram [15]. Usually, when catalytic effects are not important, alloying of an oxide with one having a smaller heat of formation increases the reduction reactivity while adding an oxide with a larger heat of formation decreases the reduction reactivity [14, 16].

In the present work the reduction of cobalt ferrite and of cobalt ferrite with aluminium in solid solution was studied. The purpose was to investigate the reduction behaviour of multi-cation oxides and the effects of a hard-to-reduce interactive dopant on the reduction behaviour. To clarify the reduction kinetics and the role of the scale in the reaction rate anomaly, the microstructures of the reduction products were characterized.

2. Experimental procedures

Dense, polycrystalline specimens of cobalt ferrite and alumina-doped cobalt ferrites* of three different compositions were used: 99.4% dense $CoFe_2O_4$, 99.5% dense $CoAl_{0.02}Fe_{1.98}O_4$, and 98.8% dense $CoAl_{0.1}Fe_{1.9}O_4$. These three materials were labelled undoped, lightly doped, and heavily doped cobalt ferrites in this paper. The

*Countis Industries, P.O. Box 1444, San Luis Obispo, California 93401, U.S.A.

rate of product layer growth was determined from optical and thermogravimetric measurements. Cube-shaped samples with edge lengths of about 0.5 cm were reacted in flowing hydrogen containing 0.01% water at a total pressure of 1 atm (1013 mbar). This gas mixture fixes the oxygen chemical potential of the reducing gas. Reaction temperatures were between 500 and 800° C, and reaction times were between 5 min and 1 h. It was found that gas velocities at the specimen greater than 1 cm sec^{-1} were sufficient to ensure that no hydrogen starvation occurred over the entire range of temperatures. The reactions were interrupted by withdrawing the specimen rapidly from the hot zone of the furnace. Kinetic data were obtained from experiments where the reaction had proceeded in a topochemical fashion. The reaction interface could be defined adequately by the use of an optical microscope at × 20 magnification. The layer growth measurements reported in this paper represent the average of three to six different reductions for each data point. Fracturing or spalling of the specimens during reduction prevented the collection of layer growth data for reactions carried out below 500° C for the undoped or lightly doped material, and below 800° C for the heavily doped material.

The reaction products were identified by X-ray diffraction, or by optical examination of chemically etched samples. Wüstite-type phases could be identified since they reacted readily with dilute hydrochloric acid while the metal phase and the spinel did not. The morphology of reduced product layers was characterized with optical and scanning electron microscopy after sectioning and polishing. One serious difficulty in the polishing of the specimen was that pull-outs occurred rather easily. This problem was most pronounced in specimens that had been reacted below 600° C. Examination of the true pore structures in reacted specimens required the removal of surface layers damaged by the polishing process. Radio frequency (r.f.) sputtering was used to mill away material to a depth of a few microns, until no further changes in scale microstructures were observed.

Weight loss kinetics were measured by thermogravimetry with a Cahn R-G electrobalance. A 19 mm diameter hangdown tube was used. The specimens were reacted in flowing hydrogen with 0.01% water at temperatures between 500 and 800° C, at a total pressure of 400 Torr (533 mbar) until the rate of weight loss was less than 1 mg in 30 min. Cube-shaped specimens were also used for these thermogravimetrical analyses. The weight-loss data can be converted to rates of scale thickening [18] provided the reaction is topochemical and there are no dimensional changes upon reduction. These two conditions were found to be satisfied.

3. Experimental results and discussion

3.1. Identification of reduction products

With X-ray analysis, only one product phase could be detected in all cases: an iron cobalt alloy. From the X-ray evidence then it would seem that under the experimental conditions used, spinel was directly transformed into metal and water vapour without undergoing an intermediate transformation through the wüstite phase. However, optical microscopy and chemical etching revealed the presence of small amounts of a (Co, Fe)O phase in reaction zones of some specimens. The relative amounts and the distribution of the wüstite found varied with reaction temperature and specimen composition. In scales of the heavily doped specimens optical microscopy revealed the presence of a dispersed, non-metallic second phase. Transmission electron microscope diffraction showed that this second phase was an iron aluminate spinel.

Aluminate-containing second-phase particles were not detected in the product scales of the lightly doped cobalt ferrites, although the presence of the aluminium ions, even in small concentration, had measurable effects on the reduction kinetics. Wüstite, observed at certain temperatures in the undoped and lightly doped cobalt ferrites, was not found in the heavily doped specimens. The details of the phase distributions are discussed below.

3.2. Layer growth kinetics

Fig. 1 shows a log–log plot of layer thickness versus time for undoped samples reacted between 600 and 800° C. The time dependences appear to be sublinear, between $t^{0.65}$ and $t^{0.75}$. Such sublinear kinetics usually indicate mixed reaction control. The use of the apparent activation energy for the purpose of determining the relative importance of the different reduction mechanisms is of little value and will not be considered. It can be found from Figs. 1 and 3 that a reaction rate anomaly occurs between 650 and 700° C. Lightly doped cobalt ferrites also show such an effect but now

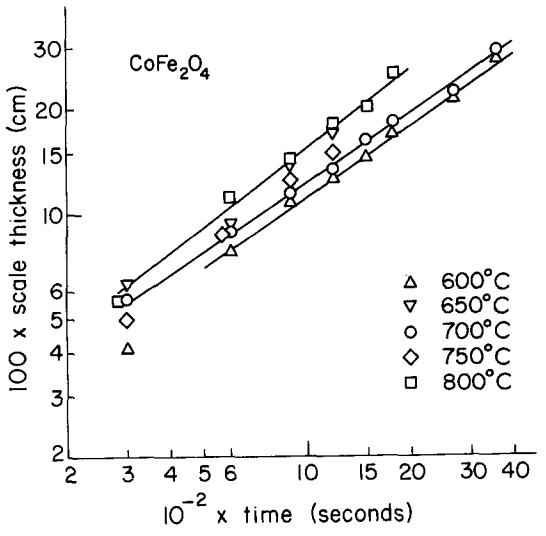

Figure 1 Log–log plot of layer growth data for undoped specimens. Note that the reaction kinetics are slower at 700° C than at 650° C. Each data point represents the simple average of three to six different reduction runs. The slopes of the lines through the data points indicate approximate time dependences of $t^{0.75}$ for the 800° C reductions and $t^{0.67}$ for the 600 and 700° C reductions. This indicates a mixed reaction control.

around 750° C, as can be found from the rate data in Figs. 2 and 3. These reaction rate anomalies have been studied in detail by Porter and De Jonghe [18], and will be reported soon.

It is interesting to note in Fig. 3 that the addition of small amounts of aluminium ions in solid solution does not uniformally decrease the reduction rates. Below 650° C, the Al^{3+}-containing

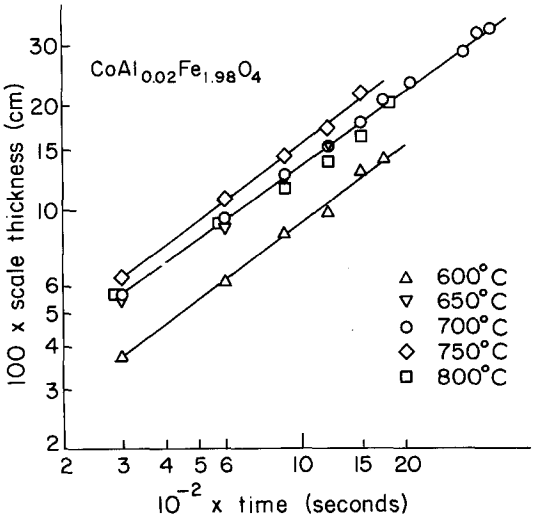

Figure 2 Log–log plot of layer growth data for lightly doped specimens. Now reaction kinetics are slower at 800° C than at 750° C.

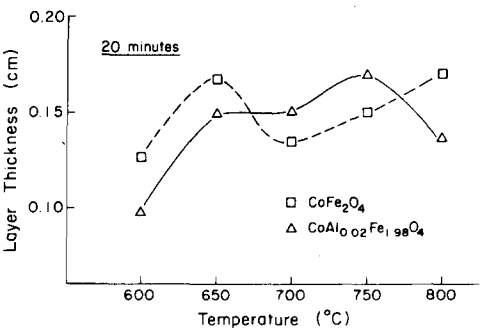

Figure 3 Comparison of undoped and lightly doped layer growth data for specimens reacted under 1 atm hydrogen for 20 min.

ferrite is reduced more slowly. Above 650° C the behaviour is more complex. The reaction rate of the undoped material decreases, while that of the lightly doped material continues to increase. Thus, the lightly doped material actually reacts faster than the undoped material between about 675 and 775° C, in the observed time interval (up to 60 min).

800° C kinetic data for undoped and heavily doped material reduced at 1 atm hydrogen are compared in Fig. 4. It is seen that the heavily doped cobalt ferrite reacts slower than the undoped one. Additional differences between the two materials were found in their scale structure.

3.3. Thermogravimetric analyses

For the thermogravimetric measurements the hydrogen pressure was 400 Torr rather than 1 atm, owing to instrument limitations. Again fissuring of the heavily doped material precluded calculating reliable layer thicknesses. The heavily doped material also showed an apparent reaction rate

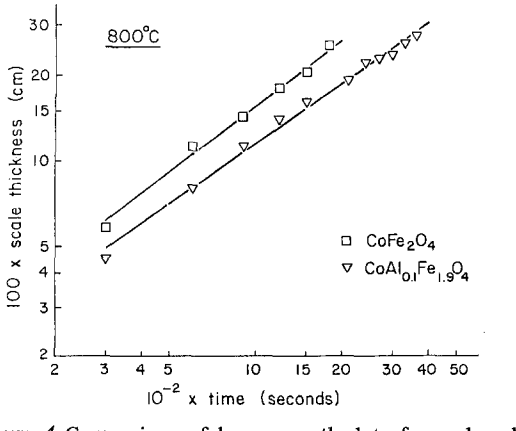

Figure 4 Comparison of layer growth data for undoped and heavily doped specimens reacted in 1 atm hydrogen at 800° C.

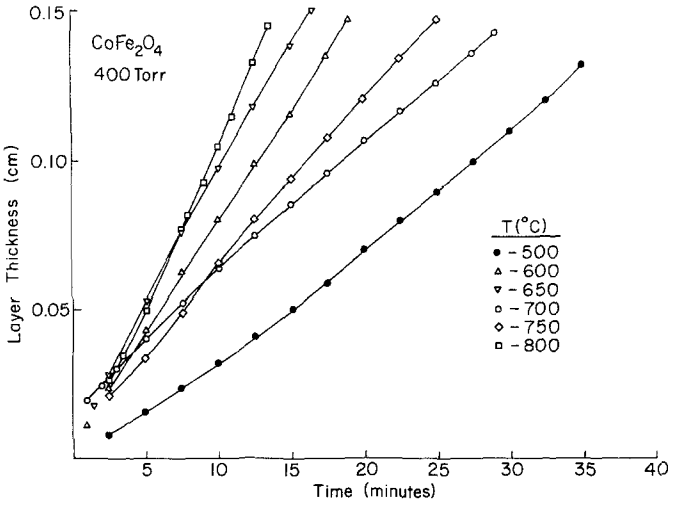

Figure 5 Layer growth data calculated from thermogravimetric data for undoped specimens.

maximum; however, this was caused by the profuse fissuring of the specimens below temperatures of 800° C.

The observed reaction rate maxima in the undoped and in the lightly doped specimens agreed in temperature with those obtained at the higher gas pressures. Apparently the maximum reaction rate temperature was not a sensitive function of the hydrogen pressure in the gas bulk, although it clearly was a sensitive function of specimen composition. Thermogravimetric data converted to rates of product layer growth are shown in Figs. 5 and 6 for undoped and for lightly doped ferrites. The general non-linearity of the layer growth kinetics indicates that the reaction is not exclusively controlled by an interface reaction.

The layer thickness calculated from the weight-loss data at fixed reduction times are shown in Figs. 7 and 8 as a function of temperature for undoped and for lightly doped specimens. Again, the reaction rate anomalies are evident. It is interesting to note that the anomalies seem more pronounced if layer thicknesses are compared at longer reduction times. This is similar to the observations reported by Turkdogan [2] for hematite ore. Some differences in reduction behaviour can be observed between the specimens reduced at 1 atm and those reduced in the thermobalance at 400 Torr. One striking difference is the degree to which the reaction rate anomally is manifested in the undoped specimen. At 1 atm hydrogen the 700° C reduction rate is higher than the 600° C rate: at 400 Torr both the 700 and 750° C rates are lower than the 600° C rate. If the internal interface reactions were of significance in controlling the reduction rates, then it would

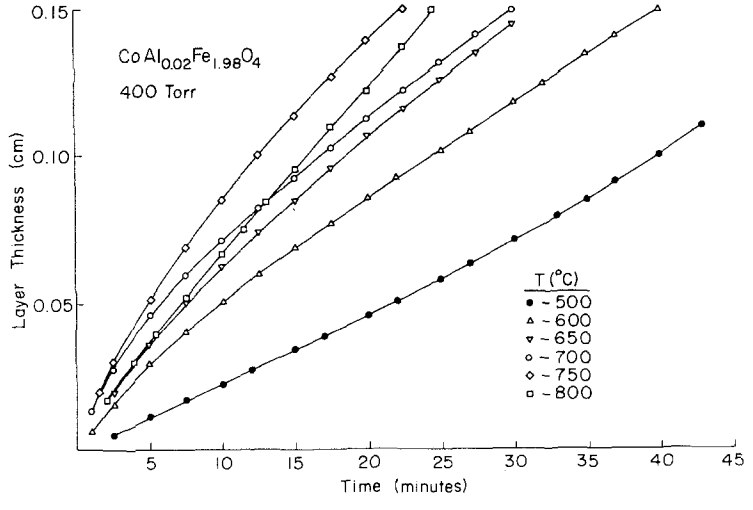

Figure 6 Layer growth data calculated from thermogravimetric data for lightly doped specimens.
mens.

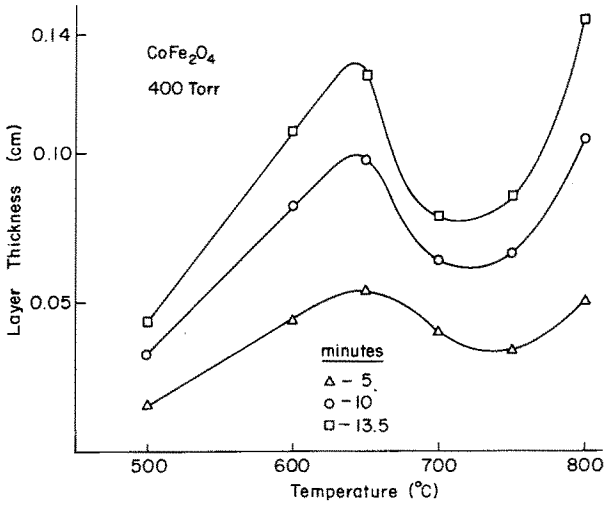

Figure 7 Reaction rate anomaly in the reduction of undoped cobalt ferrite specimens reacted in 400 Torr hydrogen. Note that the anomaly is more pronounced for longer reduction times.

appear that the gas/wüstite reaction would be more affected by the gas bulk hydrogen pressure than the gas/spinel reaction.

At 500° C the reaction kinetics shown in Figs. 5 and 6 are nearly linear. Linear growth kinetics for spherical or cubic specimens, calculated per unit area of reaction interface, usually indicate interface reaction control at the internal gas/solid interface. However, it is possible for the shell layer and gas film resistance terms to be mutually compensating so that apparently linear kinetics can result even when these two resistance terms are significant compared to the interface resistance term, as several workers have demonstrated, see, for example, [1]. If the external gas film resistance is much greater than the shell layer resistance, or vice versa, and if the larger of the two is comparable to the interfaces resistance, then the layer growth kinetics are non-linear for spherical or cubic specimens. Near-linear growth kinetics thus leaves two possibilities: predominantly interface control, or predominantly external gas film product layer resistance compensation with negligible interface resistance.

For the case of specimens of flat plate geometry, linear growth kinetics occur only when the shell layer resistance is negligible compared to the other two resistances. Thin plates of undoped cobalt ferrite have been reduced at 500° C in 400 Torr hydrogen by Porter and De Jonghe [18]. These workers observed nearly linear layer growth kinetics over a large portion of the reaction in substantial agreement with the 500° C data presented in Fig. 5. From the near-linearity of the layer growth kinetics of specimens of both flat plate and cubic geometries it can be deduced that

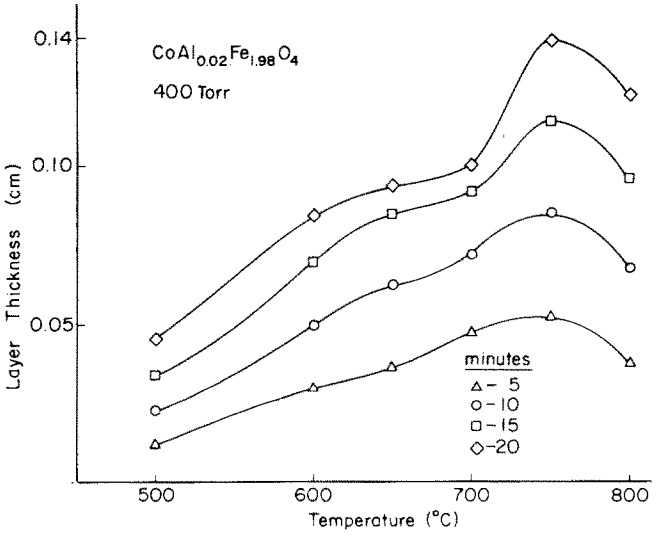

Figure 8 Reaction rate anomaly in reduction of lightly doped cobalt ferrite specimens reacted in 400 Torr hydrogen. The layer thicknesses were calculated from the thermogravimetric data.

interface reactions are mainly controlling the reduction at 500° C. The slower kinetics for the doped specimens indicate that the interface reaction resistance increases with increasing amounts of Al^{3+} in solid solution in the spinel. The increasing non-linearity of the kinetics at higher temperatures are then consistent with the gas transport resistance through the reaction product layer becoming increasingly important.

3.4. Product layer morphology

The specimen dimensions before and after reduction showed that the specimen sizes did not change measurably during the reduction. Thus, very little densification of the metal product scale occurred even at reaction temperatures as high as 800° C. The reduction product scales were therefore 48% to 50% porous. It was observed that the pore structure coarsened as a function of time (except for the heavily doped ferrites). It is not immediately clear as to why this pore coarsening is not accompanied by densification, unless surface diffusion is the dominant metal transport mode or the initial scale density is too low to permit rapid densification.

In the following, we discuss in succession the microstructure and pore structure of the scales of undoped, lightly doped and heavily doped ferrites.

3.4.1. Undoped ferrites: $CoFe_2O_4$

At 500 and 600° C, significant grain-boundary attack was observed in the undoped ferrite. Etching with hydrochloric acid showed that the cores of partially attacked grains were unreduced spinel. This mode of interface advance became more pronounced with lower reaction temperatures. This is illustrated in Fig. 9. When the individual grains have been reduced completely, loosely connected relics of the original spinel grains constitute the metal product layer. This is an example of a distributed reaction interface structure. The interface instability must arise from rapid grain-boundary reaction and slow bulk reaction. This indicates that below 600° C rapid grain-boundary diffusion of cations may play a significant role in the pronounced grain-boundary attack. If the grain-boundary cation transport rate is much higher than that of the bulk, then the excess iron ions ahead of the advancing interface can be removed, making the grain boundaries more reducible. The extent to which the interface is distributed thus depends on the grain bulk/grain-boundary cation transport rates. It is interesting to note that the overall reaction kinetics at this temperature (500° C) are quite linear, in spite of the complexity of the structure of the distributed reaction interface: as long as this distributed reaction inter-

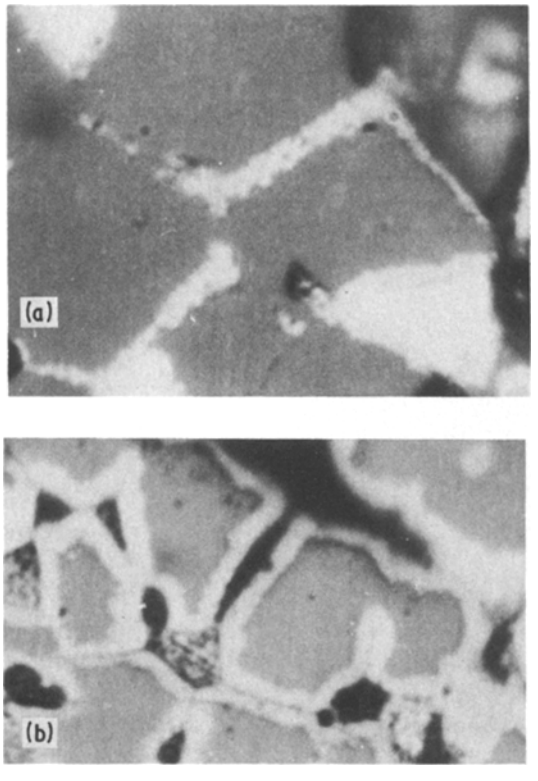

Figure 9 Microstructure near interface of undoped specimens reacted at 500° C in 1 atm hydrogen. (a) Reduction along grain boundaries. (b) and (c) show the interface region further removed from the reaction interface, changing from predominant grain-boundary attack to complete reduction. The porosity inside the grain relics in (c) is not resolved.

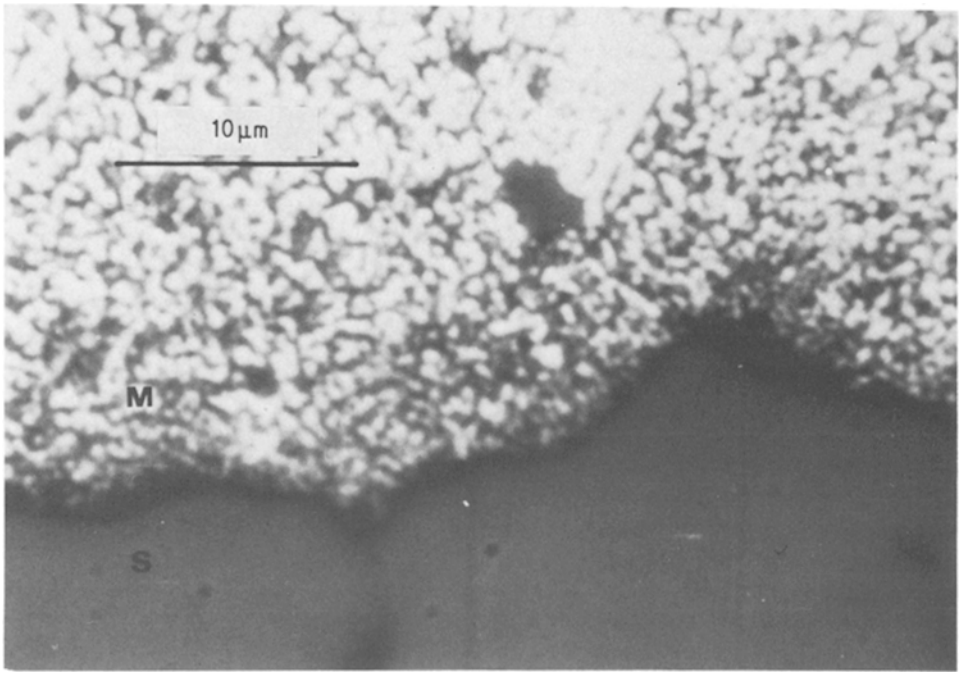

Figure 10 Optical micrograph of the interface region of an undoped specimen reacted at 700° C.

face has a steady state structure a single interface rate parameter can be used in the analysis.

At 650° C the product scale morphology changed. Extensive grain-boundary attack was no longer observed, while pore coarsening occurred to some extent in the scale. At 700° C (Fig. 10) grain-boundary attack was absent and the interface was clearly defined. Scale pore coarsening was

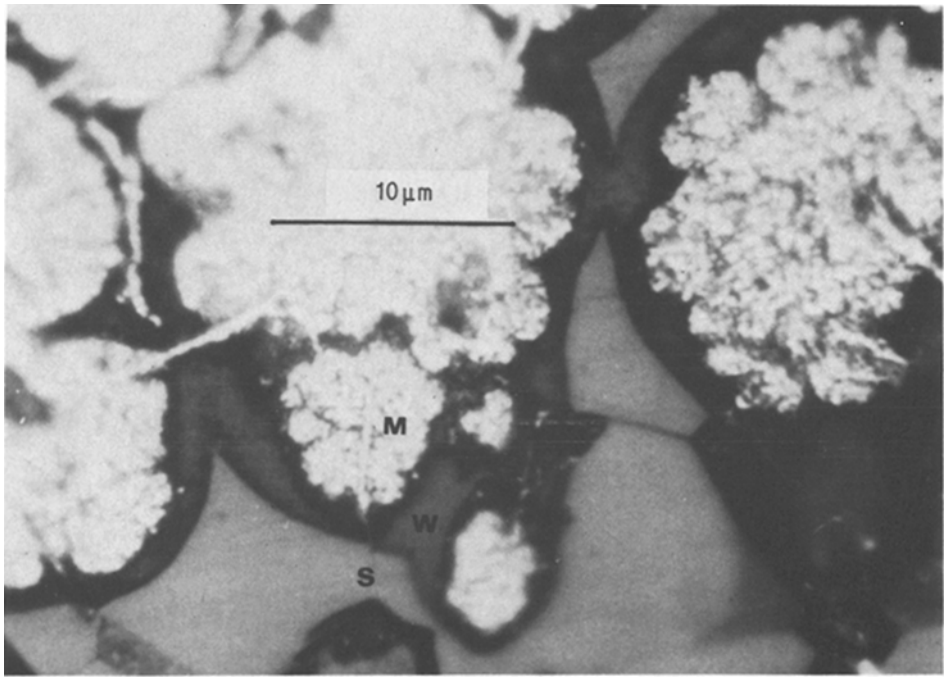

Figure 11 Optical micrograph of a slow instability in an undoped specimen reacted at 700° C. M: metal alloy; W: wüstite; S: unreduced spinel. The wüstite has been revealed by a brief etching in dilute hydrochloric acid.

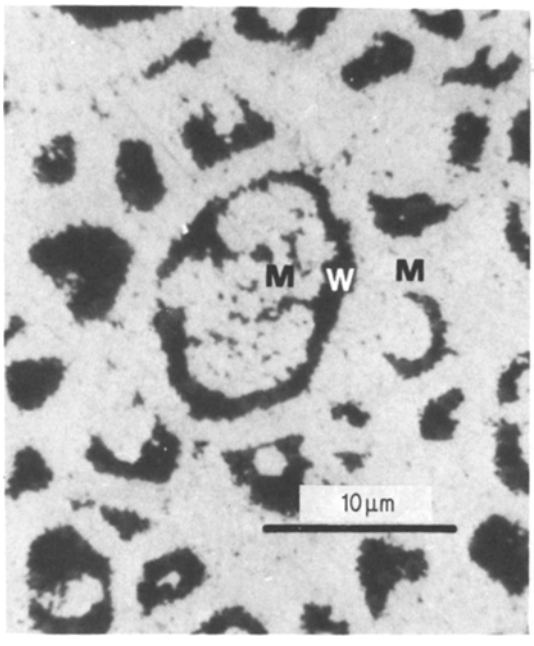

Figure 12 Retained wüstite in the metal scale at a localized slow interfacial instability in an undoped specimen reacted at 750° C.

quite evident. Optical microscopy did not detect a wüstite phase at the interface between the metal scale and the unreduced oxide, except in places – as shown in Fig. 11 – where the reaction rate had slowed down locally. Above 700° C, the interface stability was generally good, although occasionally highly localized slow instabilities were observed. One example of such an instability in a specimen reacted at 750° C is shown in Fig. 12. We note here that oxide, identified as wüstite by etching, has been retained in the scale. Again, when the reaction rate had been locally slowed the grain-boundary attack was more pronounced. Curiously, many of the wüstite grains that were retained in this scale show metal formation within the grains, in some cases separating the grain-boundary layer from the internal metal phase by a layer of oxide. This geometry probably results from the way individual grain-boundary scale instabilities are intersected in these polished cross-sections. Additionally, isolated, non-porous metal particles appeared ahead of the advancing reaction interface. Such internal reduction must involve an oxygen ion flux from the metal particle to the porous metal/oxide interface.

An example of a scale morphology resulting from reduction of undoped cobalt ferrite at 800° C is shown in Fig. 13. The pore structure in the scale is seen to evolve from being quite fine near the reaction interface, where the pore diameters are on the order of 0.1 μm, to a coarse pore structure near the specimen surface. The interface itself, while not planar, is well defined. Etching and optical microscopy again did not clearly reveal the presence of wüstite in the developing layer or in the interface region. We suspect, however, that a thin, unresolved layer of wüstite may have been present.

The pore structures of the scale could best be observed on samples that had been r.f. sputter-etched after mechnical polishing. Scanning electron micrographs of mid-scale regions of the sputter-etched samples are shown in Fig. 14. The most significant morphological changes in the scales occurred between 600 and 650° C. Up to 650° C the scale had a dual pore structure. Pores had formed along the original ferrite grain boundaries

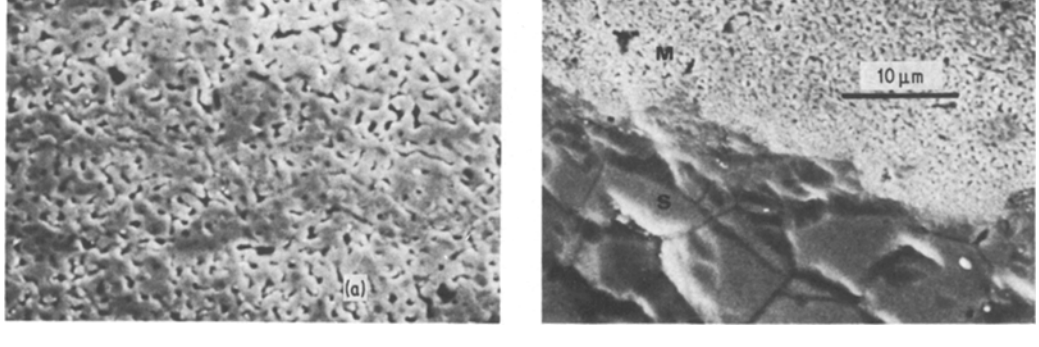

Figure 13 Scanning electron micrograph of the interface between the metal, M, and the unreacted spinel, S, of an undoped specimen reacted at 800° C in 1 atm hydrogen.

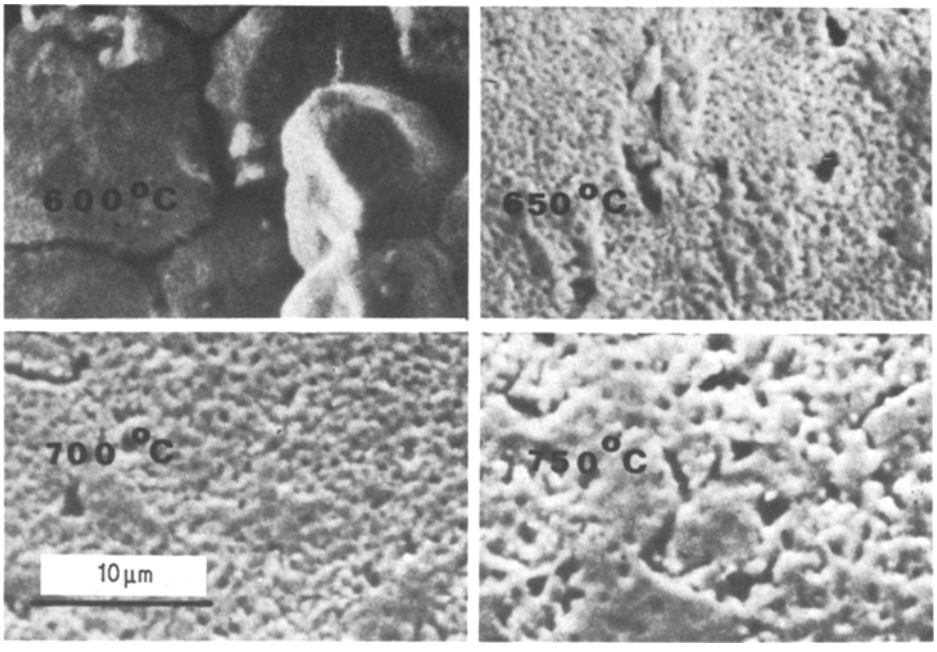

Figure 14 Pore network morphologies in the metal scales of undoped specimens at the temperature indicated. The major morpholical changes are not correlated with the reaction rate anomaly.

leaving very finely porous metal grains that were relics of the original spinel grains. The pore structure became coarser and more uniform as the temperature was increased above 650° C. Recall, however, that the total porosity was changed little since the specimens did not undergo significant dimensional changes.

3.4.2. Lightly doped ferrites: $CoAl_{0.02}Fe_{1.98}O_4$

The microstructures observed in the lightly doped specimens reduced at 500 and 600° C were much the same as those of the undoped specimens reduced at the same temperatures. At 650° C the interface was quite stable and the scale consisted of metal up to the reaction interface. Very little coarsening of the metal was observed. At 700° C the reaction interface was somewhat irregular and showed retained wüstite near the interface. The microstructure was similar to that of undoped specimens reduced at 650° C. The morphology of the scale of the lightly doped specimens reduced at 750° C closely resembled that of the slow instability of undoped specimens reduced at 750° C.

Lightly doped specimens reduced at 800° C exhibited good interface stability, while some unreduced wüstite was retained close to the interface. The pore structure of the metal layer tended to reflect the grain structure of the oxide, even after considerable coarsening. This time a subscale of wüstite, approximately 2 μm thick, could be observed at the interface. In these lightly doped specimens the appearance of the wüstite layer coincided clearly with the onset of the reaction rate anomaly. At a temperature where a continuous layer of wüstite was formed the reaction kinetics were drastically slowed.

The pore structure, revealed by r.f. sputter etching, of lightly doped material is shown in Fig. 15. The most significant changes in the pore morphology occurred well below 700° C, which rules out the possibility of attributing the reaction rate anomaly effect to changes in the pore morphology.

3.4.3. Heavily doped ferrites: $CoAl_{0.1}Fe_{1.9}O_4$

Significant grain-boundary attack was evident at all temperatures studied in heavily doped specimens, although it was much less pronounced at 800° C than at lower temperatures. The 600° C microstructure of the distributed reaction interface is partly shown in Fig. 16. The mid-scale pore structures at 600, 700 and 800° C are shown in Fig. 17. It is clear that no significant coarsening had occurred. The product metal grains remained as finely porous relics of the orignal spinel grains. We attribute the lack of coarsening to the presence

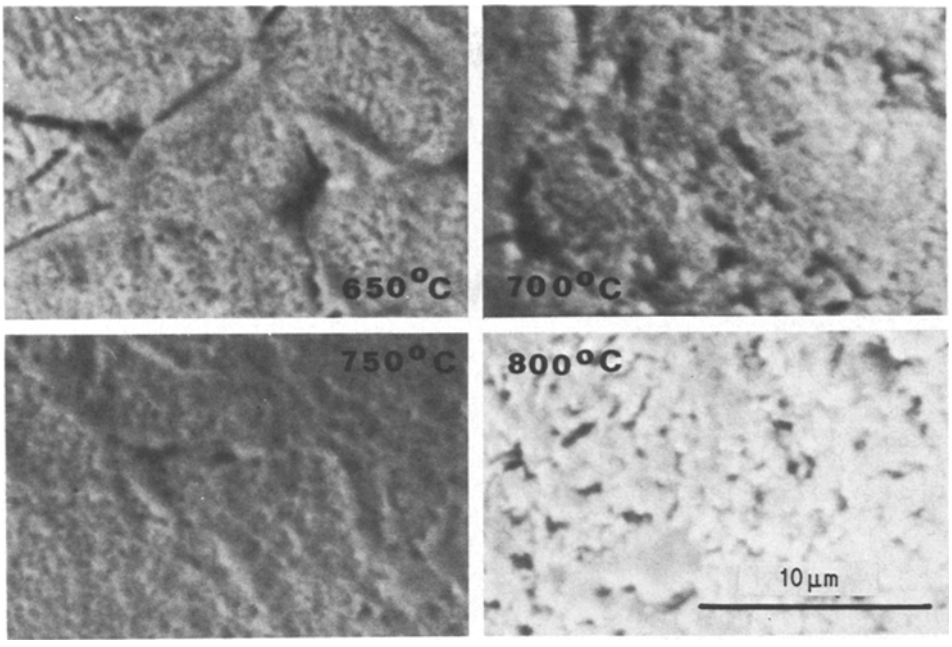

Figure 15 Pore network morphologies in the metal scales of lightly doped specimens at the temperature indicated. The specimens were sputter-etched to reveal the pore structure. No significant microstructural changes of the scale could be correlated with the reaction rate anomaly.

of the finely dispersed, unreduced aluminate phase. This dispersed phase can effectively suppress the grain-boundary movement necessary for coarsening.

4. Conclusions

(1) At 500° C hydrogen reduction of cobalt ferrite was mainly interface reaction controlled. At the same time, preferential grain-boundary attack occurred, leading to a distributed reaction interface. Above 600° C control of the reduction process was increasingly shared by the interface reaction resistance and the gas transport resistances.

(2) The reduction kinetics exhibit an anomaly. For the lightly doped material the anomalous decrease in the reaction rate around 750° C was clearly associated with the appearance of a continuous wüstite-type subscale. For the undoped material the effect at 650° C was again thought to be associated with the formation of wüstite at the metal/spinel interface, although a thin layer of

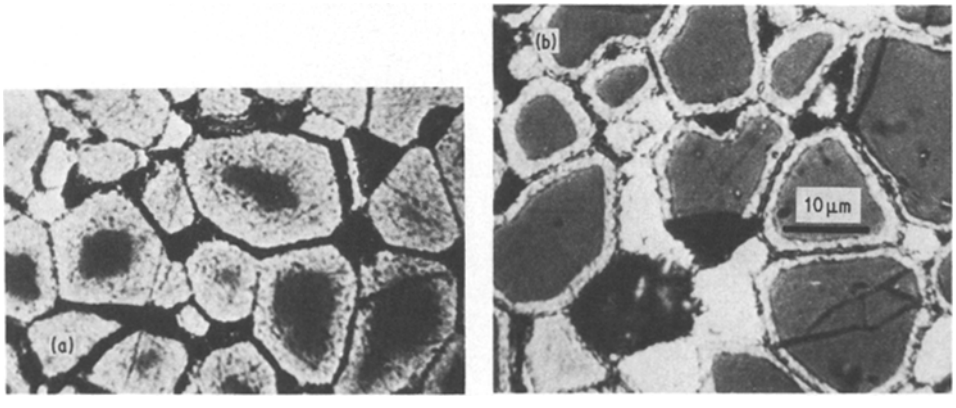

Figure 16 Distributed reaction interface of heavily doped specimen reacted at 600° C. The width of the total reaction interface is on the order of 100 μm (a) is towards the outside of the reaction zone while (b) is towards the inner region of the reaction zone. The individual grains now behave as particles for which the shrinking core model [6] could be applied again.

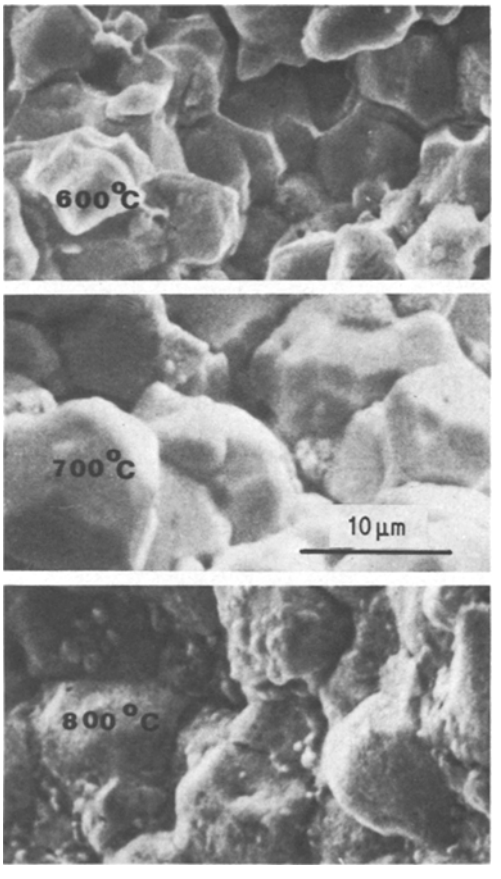

Figure 17 Pore morphology in metal scales of heavily doped specimens at 600, 700 and 800° C. The sintering of the metal scale has been completely inhibited by the presence of finely dispersed unreduced iron aluminate particles.

(Co, Fe)O was not clearly detected by optical microscopy.

(3) The main micromorphological changes in the porous product layer were not associated with reduction rate anomaly.

(4) Substitution of aluminium ions for iron ions in cobalt ferrite significantly altered the reduction kinetics. Important effects were the lowering of the interface reaction rates and the inhibition of coarsening of the metal product layer by the finely dispersed unreduced aluminates. The presence of Al^{3+} shifted the appearance of the anomalous reaction rate decrease to a higher temperature.

5. Acknowledgements

A significant part of this work was carried out under DOE contract EY-76-5-02-2584 at Cornell University. Part of this work was also supported by the Basic Science Division of the US Department of Energy under contract no. W-7405–ENG-48.

References

1. R. H. SPITZER, F. S. MANNING and W. O. PHILBROOK, *Trans. Met. Soc. AIME* **236** (1966) 726.
2. E. T. TURKDOGAN and J. V. VINTERS, *Met. Trans.* **2** (1971) 3175.
3. J. E. EDSTRÖM, *J. Iron Steel Inst* **175** (1953) 289.
4. M. C. UDY and C. H. LORIG, *Trans. Met. Soc. AIME* **154** (1943) 162.
5. J. HENDERSON, *J. Austr. Inst. Met.* **7** (1962) 115.
6. J. SZEKELY and J. W. EVANS, *Chem. Eng. Sci.* **26** (1971) 1901.
7. K. R. LILIUS, *Acta Polytec. Scand* **118** (1974) 6.
8. B. DELMON, "Reactivity of Solids", Vol. 7 (Chapman and Hill, London, 1972) pp. 567-75.
9. E. AUKRUST and A. MUAN, *Trans. Met. Soc. AIME* **230** (1964) 1395.
10. N. I. IL'CHENKO and V. A. YUZA, *Kin. Katal.* **2** (1966) 118.
11. W. VERHOEVEN and B. DELMON, *Compt. Rend. Aca. Sci. Paris* **262C** (1966) 33.
12. W. MACHU and S. Y. EZZ, *Arch. Eisenhuttenw.* **28** (1957) 367.
13. D. K. LAMBIEV, T. M. ATANASSOV and O. B. STOIMENOV, *Dokl. Bulg. Akad. Nauk* **27** (1979) 1675.
14. M. H. TIKKANEN, B. O. ROSELL and O. WIBERG, *Acta Chem. Scand.* **17** (Ab3) 513.
15. E. AUKRUST and A. MUAN, *Trans. Met. Soc. AIME* **230** (1964) 1378.
16. Y. LIDA and K. SHIMADA, *Bull. Chem. Soc. Japan* **33** (1960) 8.
17. W. M. McKEWAN, *Trans. Met. Soc. AIME* **218** (1960) 2.
18. J. PORTER and L. C. DE JONGHE, Lawrence Berkeley Laboratory Report LBL-9801, June (1979) *Met. Trans. B* (1980).

Received 3 January and accepted 29 January 1980.